

Title	Forced flow boiling heat transfer properties of liquid hydrogen for manganin plate pasted on one side of a rectangular duct
Author(s)	Yoneda, K.; Shirai, Y.; Shiotsu, M.; Oura, Y.; Horie, Y.; Matsuzawa, T.; Shigeta, H.; Tatsumoto, H.; Hata, K.; Naruo, Y.; Kobayashi, H.; Inatani, Y.
Citation	Physics Procedia (2015), 67: 637-642
Issue Date	2015
URL	http://hdl.handle.net/2433/215134
Right	© 2015 Published by Elsevier B.V. This is an open access article under the CC BY-NC-ND license(http://creativecommons.org/licenses/by-nc-nd/4.0/).
Type	Journal Article
Textversion	publisher

25th International Cryogenic Engineering Conference and the International Cryogenic Materials Conference in 2014, ICEC 25–ICMC 2014

Forced flow boiling heat transfer properties of liquid hydrogen for manganin plate pasted on one side of a rectangular duct

K. Yoneda^{a*}, Y. Shirai^a, M. Shiotsu^a, Y. Oura^a, Y. Horie^a, T. Matsuzawa^a, H. Shigeta^a, H. Tatsumoto^b, K. Hata^c, Y. Naruo^d, H. Kobayashi^d, Y. Inatani^d

^a Dept. of Energy Science & Technology, Kyoto University, Sakyo-ku, Kyoto, Japan

^b J-PARC Center, Japan Atomic Energy Agency, Tokai, Ibaraki, Japan

^c Institute of Advanced Energy, Kyoto University, Uji, Kyoto, Japan

^d Institute of Space and Astronautical Science, JAXA, Kanagawa, Japan

Abstract

In this report, we show results on the forced flow boiling heat transfer experiments for manganin plate pasted on one side of a rectangular duct. Nucleate boiling heat transfer and its Departure from Nucleate Boiling (DNB) heat flux were measured for various pressures, subcooling and flow velocities. The DNB heat fluxes are higher for higher subcooling and higher flow velocity. The DNB heat fluxes were compared with the experimental data for round tube of nearly equal equivalent diameter. The DNB heat fluxes for the rectangular duct are lower than those for the round tube.

© 2015 Published by Elsevier B.V. This is an open access article under the CC BY-NC-ND license

(<http://creativecommons.org/licenses/by-nc-nd/4.0/>).

Peer-review under responsibility of the organizing committee of ICEC 25-ICMC 2014

Keywords: Liquid Hydrogen; Forced Flow; Heat Transfer

1. Introduction

Liquid hydrogen has excellent properties as a coolant such as large latent heat, low viscosity and so on. Therefore liquid hydrogen is expected to be a coolant for high critical temperature superconducting devices. In order to design

* Corresponding author. Tel.: 81-75-753-9180

E-mail address: yoneda@pe.energy.kyoto-u.ac.jp

superconducting devices cooled by liquid hydrogen, it is necessary to understand the cooling characteristics of forced flow liquid hydrogen. Forced flow boiling heat transfer of liquid hydrogen from inner side of heated tubes with several diameters and lengths have been studied under wide range of experimental conditions [1,2]. However there would be many shapes of liquid hydrogen flow passages and heated surfaces in actual superconducting devices.

We designed and made the test plate heater of manganin pasted on one side of a rectangular duct made of FRP (Fiber Reinforced Plastic) block, and forced flow boiling heat transfer properties of the test heater were measured. In this report, we show the results of the experiments and compare them with the results on the past experiments for the tube heater.

2. Experimental apparatus and method

The schematic diagram of the experimental system is shown in Fig. 1. The system has a main cryogenic tank, a sub cryogenic tank, hydrogen transfer tube with a flow control valve and feed hydrogen gas line.

The apparatus is installed in an explosion-proof room. LH₂ container and GH₂ curdle are set outside, and electric power source to supply heat input to the test heater is also set next to the explosion proof room. During the experiments, the experimental system is remotely operated in a control room about 100 m away from the experimental field.

The main tank is connected to the sub tank through the hydrogen transfer tube with the flow control valve (CV001). The main tank is pressurized to a desired pressure by pure hydrogen gas, and the pressure is controlled by the dome loaded gas regulator. On the other hand the sub tank is always maintained to be atmospheric pressure. The pressure difference and the open ratio of CV001 produce forced flow of LH₂ from the main tank to the sub tank through the hydrogen transfer tube. A test heater is located at one end of the transfer tube in the main tank. There is a scale under the main tank, the mass flow velocity is measured by the weight change of the main tank. The inlet liquid temperature is measured by Cernox temperature sensor with the accuracy of 10 mK.

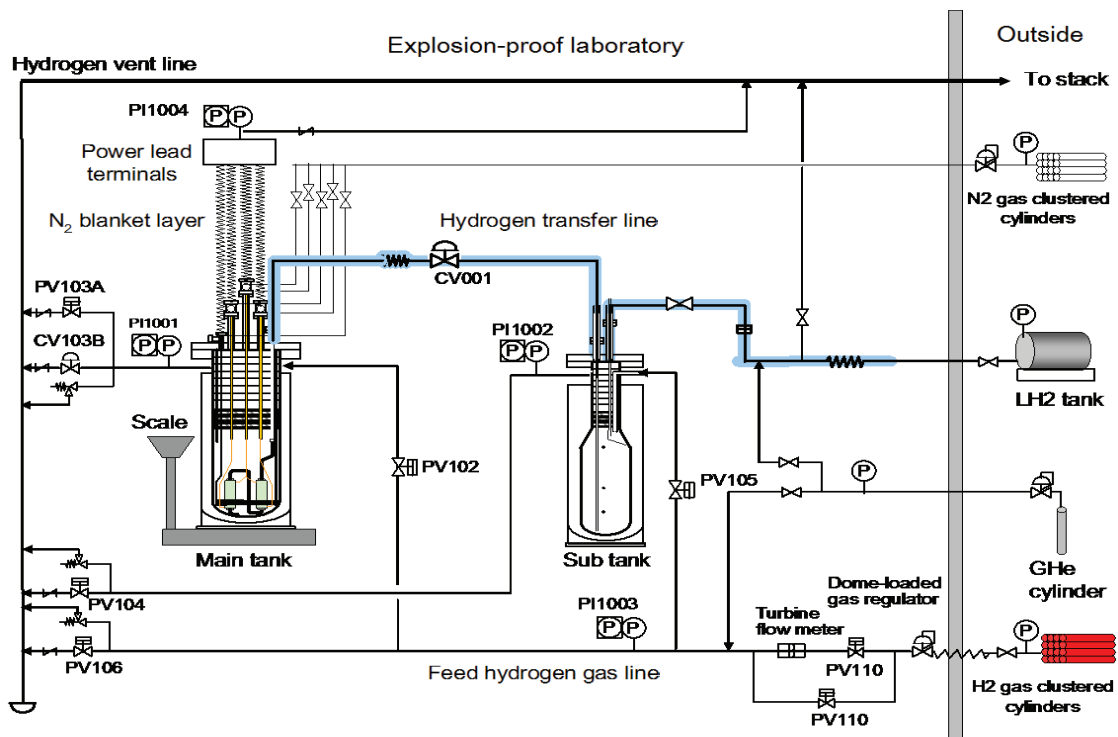


Fig. 1. Schematic diagram of the experimental system.

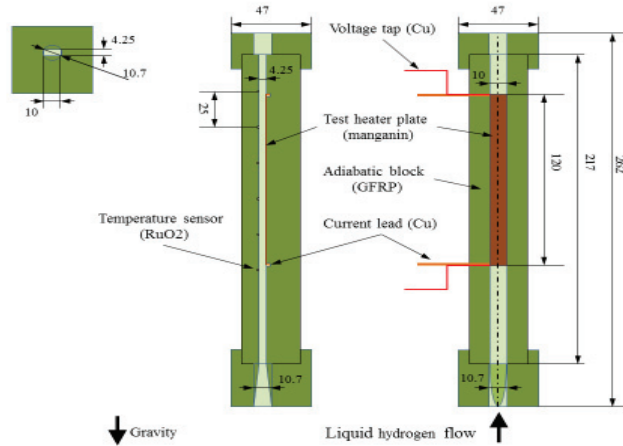


Fig. 2. Schematic diagram of the test heater.

The schematic of the test heater is shown in Fig.2. The test heater is a manganin plate pasted on one side of a rectangular duct made of FRP with 4.2mm × 10mm in cross section. The manganin plate heater is 10 mm wide, 120 mm long and 0.1 mm thick. The flow channel gradually changes to a rectangle from the round transfer tube. The support running distance of 69 mm is provided before the heater in order to stabilize the LH₂ flow.

In addition, six Ruthenium-Oxide (RuO₂) temperature sensors of 0.3 mm × 0.5 mm × 1.0 mm are attached in small holes on the FRP opposite side of the heater in the rectangular duct.

The following is the experimental process. At first the main tank was pressurized to a desired pressure, which produced LH₂ flow from the main tank to the sub tank. The CV001 was open to a curtain rate. When the flow rate became constant, heating current was supplied to the test heater. The exponentially increasing heat input Q_L was given as following:

$$Q_L = Q_0 \exp\left(\frac{t}{\tau}\right). \quad (1)$$

In these tests, the heat generation rate Q_L expressed in Eq.(1) with $\tau = 5$ s was applied to the test heater. In past experiments, we had given heat input expressed in Eq.(1) to another heater with several heat generation rate and obtained each boiling curve. The boiling curves had been almost same with comparatively small heat generation rate such as $\tau = 10, 5, 2$ s. So it had been experimentally confirmed that the heat transfer phenomenon at this heat generation rate could be regarded as a continuous series of steady state. The average temperature of the test heater was calculated by electrical resistivity of it after the measurement. The heat transfer from the plate heater was measured for the inlet temperatures from 20.6 K to each saturated temperature T_{sat} at the pressures of 0.4, 0.7, 1.1 MPa. The flow velocity was varied from about 0.3 to 15 m/s.

3. Results and discussion

The typical result of boiling curves under saturated condition is shown in Fig.3 with flow velocity as a parameter at the pressure of 0.7 MPa. The vertical axis is the heat flux q , the horizontal axis is the heater surface superheat, $\Delta T_{sat} = T_s - T_{sat}$. T_s means the average surface temperature. The solid lines show the experimental results, the broken lines show the curves predicted by the Dittus-Boelter equation [3], where hydraulic equivalent diameter was used as a representative length.

At first as the heat input increases, the heat flux, q , gradually increases along the curve predicted by the Dittus-Boelter equation.

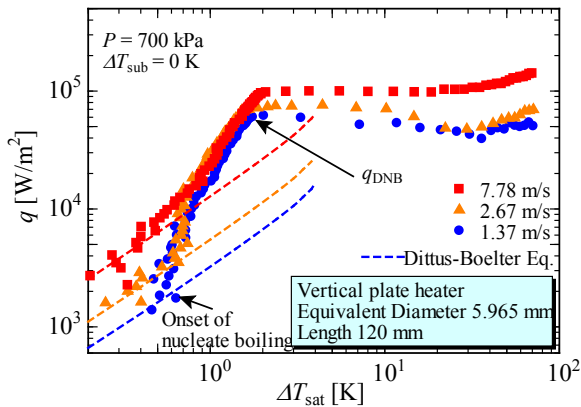


Fig. 3. Boiling curves for various flow velocities at the pressure of 0.7 MPa under saturated condition.

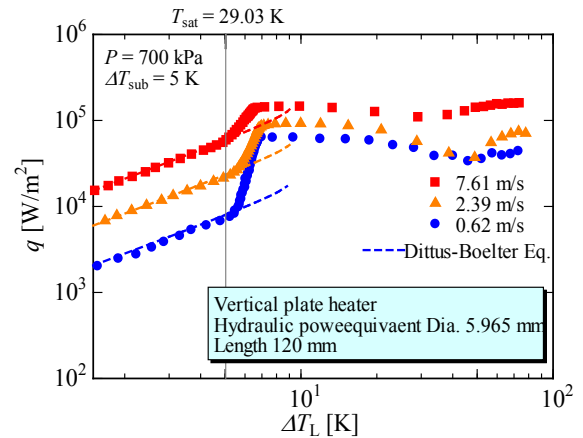


Fig. 4. Boiling curves for various flow velocity at the pressure of 0.7 MPa under sub-cooled condition, $\Delta T_L = 5$ K.

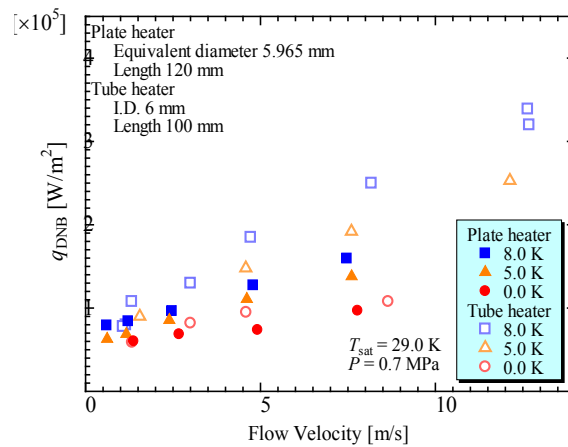


Fig. 5. DNB heat flux versus flow velocity at the pressure of 0.7 MPa for various subcooling.

Then there are points where the ratio of the heat flux increasing becomes higher. It seems to be the onset of nucleate boiling. In the nucleate boiling region, the heat flux increases largely with the slight increase of ΔT_{sat} up to DNB heat flux, q_{DNB} . After the heat flux reaches q_{DNB} , ΔT_{sat} rapidly increases. The boiling phenomenon jumps to film boiling region. In the beginning of film boiling region, the heat flux q decreases slightly. This would be because transition to film boiling first occurs near the outlet, but the surface temperature of the heater is calculated by the average temperature in longer direction.

Next, the typical result of boiling curves under sub-cooled condition $\Delta T_{sub} = 5$ K at the pressure of 0.7 MPa is shown in Fig. 4 with flow velocity as a parameter. The horizontal axis is the difference between the heater surface temperature and the inlet liquid temperature of the flow channel, ΔT_L .

With an increase of ΔT_L by heat input, the heat flux gradually increases along the curve predicted by Dittus-Boelter equation. After the heater surface temperature reached the saturated temperature, nucleate boiling begins and the heat flux rapidly increases with slight increase of ΔT_L up to the DNB heat flux. In non boiling region and nucleate boiling region, the heat flux is higher for higher flow velocity. The DNB heat flux is also higher for higher flow velocity.

The DNB heat fluxes of the test heater were obtained for various pressures, sub-cooling states and flow velocities. The typical result of the DNB heat flux at the pressure of 0.7 MPa is shown versus flow velocity in Fig. 5 with

subcooling, ΔT_{sub} as a parameter. Fig. 5 also shows the experimental data for round tube heater of nearly equal equivalent diameter and length [1] in order to compare with them.

The DNB heat flux is higher for higher flow velocity and subcooling. The DNB heat flux for the plate heater is lower than that for the tube heater under most conditions.

In nucleate boiling near the DNB heat flux, there would be a lot of bubbles on the heater surface in the rectangular duct. The friction between LH₂ flow and the heater surface would be rather small owing to the bubbles. So LH₂ could easily flow along heated surface. On the other hand, there would be few vapor bubble on another unheated sides of the duct. Due to the viscosity of LH₂, the flow velocity on the unheated surface of the duct would be zero.

The section around the side corners of the duct on the heater surface is the boundary between heated and unheated surfaces of the duct. So the flow velocity around both side walls of the duct would be lower than other parts of the heated surface. This may cause locally lower DNB heat flux.

4. Liquid temperature distribution

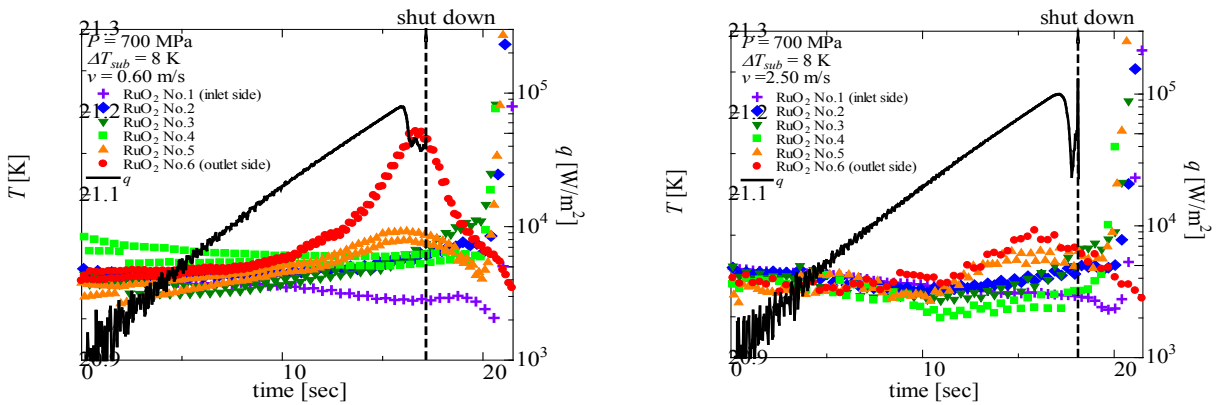
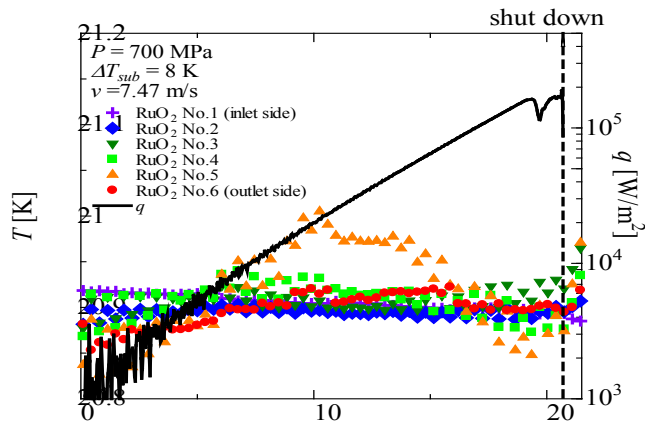


Fig. 6. (a) Liquid temperature distribution with flow velocity of 0.60 m/s; (b) Liquid temperature distribution with flow velocity of 2.50 m/s;



(c) Liquid temperature distribution with flow velocity of 7.47 m/s.

Information of the liquid temperature distribution on the non-heated plate opposite to the heater may be helpful to see the growth of thermal boundary layer on the heater.

The liquid temperature was measured with six RuO₂ temperature sensors which had been calibrated from 20.4 K to 32 K before all experiments. As a matter of convenience, we assigned numbers from 1 to 6 to the six RuO₂ temperature sensors in order from the inlet side to the outlet side.

The typical results of liquid temperature distribution at the pressure of 0.7 MPa under sub-cooled condition, $\Delta T_{sub} = 8$ K with flow velocity of 0.6, 2.5 and 7.47 m/s are shown in Fig. 6(a), Fig. 6(b) and Fig. 6(c), respectively. The vertical axis on the left is the temperature given by RuO₂ temperature sensors, and that on the right is the heat flux. The horizontal axis is elapsed time.

In Fig. 6(a), the temperature of the nearest and second nearest RuO₂s to the outlet, that is No. 6 and No.5, increase as heat flux increases. Then after the power supply is shut down, the temperature of them begin to decrease gradually. The temperature of RuO₂ No. 6 rises up the highest, and that of RuO₂ No. 5 rises up the second highest. Under forced flow condition, nearer part of the heater to the outlet of the flow channel would start to jump to film boiling earlier.

On the other hand, the other RuO₂s start to rise up after the power supply was shut down, and the ratio of temperature increase of the RuO₂ No. 3 is the largest. Forced flow of LH₂ was stopped at the same time as the power supply was shut down. After the forced flow of LH₂ was stopped, backflow of LH₂ would occur. So the temperature of RuO₂s seems to rise up in order from the outlet to the inlet. The experimental data shown in Fig. 6(b) with flow velocity of 2.50 m/s is noisier than that in Fig. 6(a) with flow velocity of 0.60 m/s, but it shows similar trend of liquid temperature distribution to that in Fig. 6(a). However the experimental data in Fig. 6(c) with flow velocity of 7.47 m/s is much noisier and shows that the temperatures of all RuO₂s hardly change. This result shows that the thermal boundary layer is thinner for higher flow velocities, and then the layer does not reach the opposite side of the heater.

5. Conclusion

Forced flow boiling heat transfer properties and the DNB heat flux were measured for the manganin plate pasted on one side of a rectangular duct. Experimental results lead to the following conclusions.

- Non-boiling heat transfer coefficients are well described by the Dittus-Boelter equation.
- The DNB heat flux is higher for higher flow velocity and subcooling.
- In comparison with the experimental data for a round tube heater of nearly equal equivalent diameter, the DNB heat flux for the plate heater is lower than that for the tube heater under most conditions.

The reason may be due to lower flow velocity at the corner part of heated and unheated sections. Additional experiments for another plate heater need to be carried out in order to confirm the assumption.

- Liquid temperature distribution on the unheated side was measured by RuO₂ temperature sensors. The temperature nearer to the outlet of the flow channel rises up higher under condition that flow velocity is comparatively lower.

Thermal boundary layer is thinner for higher flow velocities. The layer does not reach the opposite side of the heater for the highest flow velocity of 7.47 m/s.

References

1. Shirai, Y., Shiotsu, M., Kobayashi, H., Takegami, T., Tatsumoto, H., Hata, K., Kobayashi, H., Naruo, Y., Inatani, Y., Kinoshita, K., 2012, in "Advances in Cryogenic Engineering vol. 57", 1067-1074.
2. Tatsumoto, H., Shirai, Y., Shiotsu, M., Hata, K., Naruo, Y., Kobayashi, H., Inatani, Y., Kinoshita K., 2012, in "Advances in Cryogenic Engineering vol.57", 747-754.
3. Van Sciver, S. W., Helium Cryogenics, Plenum Press, New York, 1986, 251.